



Research Article

Platelet Rich Plasma (PRP) Treatment: A Viable Treatment for Myocardial Ischemic Reperfusion Injury

Barbara Hargrave^{1*} and Frank Lattanzio²

¹Professor, Center for Bioelectronics and College of Sciences, USA

²Professor, Department of Biomedical and Translational Sciences Macon & Joan Brock, Virginia Health Sciences at Old Dominion University, Norfolk, Virginia, 23508, USA

Submitted : 20 March, 2026

Accepted : 01 April, 2026

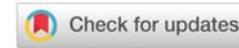
Published : 02 April, 2026

*Corresponding author: Dr. Barbara Hargrave, Professor, Center for Bioelectronics and College of Sciences, USA, E-mail: bhargrav@odu.edu

Keywords: Myocardial ischemia-reperfusion injury; Platelet-rich plasma; Reactive oxygen species; Oxidative stress; Nrf2 signaling pathway; Heat shock proteins

Copyright License: © 2026 Hargrave B, et al. This is an open-access article distributed under the terms of the Creative Commons Attribution License, which permits unrestricted use, distribution, and reproduction in any medium, provided the original author and source are credited.

<https://www.organscigroup.com>



Abstract

Myocardial infarction and several surgical and vascular procedures contribute to MIRI. Research has primarily focused on the restoration of blood flow to the ischemic tissue. However, an inherent response to restoring blood flow to heart tissue after ischemia is reperfusion injury generated in part by an increase in the production of reactive oxygen species (ROS). Platelet-rich plasma (PRP) is a promising treatment for supporting cardiomyocytes exposed to MIRI and oxidative stress. We assessed the effects of PRP in the presence or absence of the NOX-2 or NOX-4 inhibitors using the rabbit Langendorff heart method of MIRI and in cardiac myoblast cells (H9c2) and Adipose Derived Stem Cells (ADSC) exposed to hypoxia. Left ventricular systolic (LVSP), diastolic (LVDP), and work function (LVWF) were analyzed in the Langendorff hearts. The ROS concentration, hypoxia-inducible factor 1-alpha activity, and channel formation were analyzed in cardiac myoblast cells, *in vitro*.

Introduction

Myocardial ischemia reperfusion injury (MIRI) secondary to myocardial infarction contributes to death and disability [1,2]. MIRI can also occur from several standard medical and surgical procedures, including cardiothoracic and vascular surgeries and organ transplantation [3,4]. Due to the worldwide morbidity and mortality associated with cardiovascular disease, research has primarily focused on the restoration of blood flow to the ischemic tissue. However, an inherent response to restoring blood flow to heart tissue after ischemia is reperfusion injury.

Reperfusion injury is a complicated process that is mediated, at least in part, by an increase in reactive oxygen species (ROS) to the extent that an imbalance occurs between ROS production and the cell's ability to defend itself against damage. Currently, attention is being paid to treatments that can protect cardiac myocytes adjacent to, but may not be involved in, the infarct zone from responding to the increase in ROS by undergoing apoptosis and death. Reoxygenation of the ischemic lesion

causes a robust production of ROS and ROS damage to heart cells. In the heart, ischemia occurs when there is a decrease in oxygen content, causing a switch in cellular metabolism from aerobic to anaerobic respiration [5].

Platelet Rich Plasma (PRP) is a promising treatment that can potentially protect cardiac myocytes from ischemic reperfusion damage by lowering oxidative stress. PRP contains growth factors and proteins stored within the alpha granules of red blood cells that are released upon platelet activation. PRP has been reported to reduce ROS by modulating cellular signaling pathways, activating antioxidant defenses via the nuclear factor erythroid-2 related factor (Nrf2) system, and directly providing antioxidant enzymes and protecting mitochondria. The Nrf2 pathway is a key regulator of the antioxidant response, leading to increased production of superoxide dismutase (SOD) and catalase [6]. In a previous study, using cardiac myoblast cells in culture, we reported that catalase and SOD were present in greater concentrations in PRP than in the vehicle used to treat the cells under oxidative stress



[7]. While PRP lowered ROS levels in our previous studies, it did not reduce them to zero, thereby maintaining a required minimal level of ROS [8]. A minimum level of ROS is necessary for activation of proteins such as Hydroxylated-HIF-1 α (HIF-1 α) and inhibition of Peroxisome Proliferator-Activated Receptor- α (PPAR α) during MIRI [9]. In addition to its harmful effects on cardiomyocytes, ROS plays a physiological role in the heart under stress. A small amount of ROS plays a protective role against MIRI by inducing preconditioning [10]. Basal levels of ROS derived from the nicotinamide adenine phosphate (NADPH) oxidases, either NOX-2 or NOX-4, are required to maintain homeostasis in the heart during MIRI.

In addition to activation of the Nrf2 signaling pathway reported by Togonlini, et al., we have previously demonstrated that PRP increases the activity of the heart-protective heat shock proteins (Hsps) 20 and 70 [11]. Consistent with this data, Hu et al have shown that the activity of Hsps can minimize the cellular damage occurring in the response to oxidative stress. The expression of Hsp 70 in cardiomyocytes protects the cells and heart tissue from oxidative stress and has anti-apoptotic potential related to the inhibition of caspase 3 [12]. Also, Kayama, et al. demonstrated the cardiomyocyte-protection activity of Hsp 70 by showing that Hsp 70 inhibited ROS production and its mediated damage in cardiomyocytes [13].

Like other investigators, we have investigated the use of PRP as a method to reduce ROS levels and support left ventricular mechanical and electrical function under ischemic and reperfusion conditions. Our *in vitro* evidence shows that PRP lowers ROS and is associated with less mitochondrial depolarization in H9c2 cardiac myoblast cells in culture, stressed with hydrogen peroxide [8]. Using optical mapping of the Langendorff rabbit heart, we have also provided evidence that in rabbit hearts injected with PRP, recovery of electrical activity after ischemia and reperfusion occurred more rapidly [11], suggesting that PRP may be involved in gap junction formation in its support of cardiac function.

Under basal conditions, the heart primarily uses fatty acids as a substrate to produce ATP. However, during hypoxia, glycolytic genes are upregulated by HIF-1 α to maintain ATP production, reduce further increases in ROS, and inhibit fatty acid oxidation (FAO) by suppressing PPAPs in the heart. The primary function of HIF-1 α during hypoxia is to help the body adapt to the low oxygen environment by increasing oxygen delivery, energy production, and cell survival [14]. In response to hypoxia, HIF-1 α becomes stabilized and translocated to the cell nucleus, where it binds to specific DNA sequences (HREs) to activate the transcription of target genes. HIF-1 α promotes the switch to anaerobic metabolism (glycolysis), allowing cells to generate energy even without sufficient oxygen [15].

While there are several sources of ROS production during MIRI, such as xanthine oxidase, cytochrome oxidase, cyclooxygenase, fatty acid oxidation, and mitochondrial oxidation, this work will investigate the effects of PRP on ROS levels in the presence and absence of the NADPH oxidases NOX-2 and NOX-4. NADPH oxidases are a family of enzymes whose main function is to produce ROS. NOX-2 is an inducible enzyme located primarily on the plasma membrane [16], and

NOX-4 is constitutively active and is regulated by its expression levels. NOX-4 is in the mitochondria, endoplasmic reticulum, and the nucleus [17-19].

The functions of endogenous NOX-2 and NOX-4 during MIRI have been investigated using NOX isoform-specific knockout (KO) mice. However, the data describing the detrimental roles of NOX isoforms during MIRI is mixed. Some of the data showed a significant decrease in infarct size after MIRI in NOX-2 KO mice but not in NOX-4 KO mice [20,21], while others found no attenuation in MIRI in mice [22]. The observed functions of NOX-4 are reported to have protective effects in endothelial cells [23] by attenuating inflammation and enhancing angiogenesis [23], but overexpression of NOX-4 in cardiomyocytes promotes apoptosis *in vitro* [24]. Interestingly, in single KO mouse hearts where NOX-2 or NOX-4 is knocked down after MIRI, HIF-1 α and PPAR α are preserved.

Critical to heart function is the presence of gap junctions. Gap junctions or cell-to-cell channels are ion channels different from voltage-gated and ligand-gated ion channels [25]. Smyth, et al. report that after cardiac insult, gap junction coupling occurs rapidly, with the rapid movement of connexons to the plasma membrane [26]. Gap junctions in the heart form a communication connection between cardiac cells to ensure the propagation of electrical impulses so that one cell functions synchronously with another cell. In this study, we investigated the effects of PRP on the formation of channels (gap junctions) *in vitro* under hypoxic conditions [27].

According to Kaur, et al., the coronary no-reflow phenomenon is a lethal mechanism of ongoing myocardial injury following successful revascularization of an infarct-related coronary artery and is associated with adverse hospital and long-term outcomes and a high occurrence of failure following percutaneous intervention [28]. Dil, et al. have reported that microvascular obstruction (no-reflow phenomenon) and increased left ventricular end-diastolic pressure are implicated in the pathogenesis and exacerbation of ischemic injury in the heart [29]. Therefore, it is clinically significant to develop cardio-protective agents such as PRP that can adjust the concentration of ROS, causing less damage to the endothelial coronary microvasculature, which is theorized to be associated with the no-reflow phenomenon [25].

In this study, we will focus on the effects of PRP during MIRI when NOX-2 and/or NOX-4 are inhibited. Left ventricular systolic pressure (LVSP), left ventricular diastolic pressure (LVDP), and left ventricular work function (LVWF) will be monitored after ischemic damage and during reperfusion in the Langendorff heart model of MIRI. We will also investigate the *in vitro* effects of PRP on gap junction formation, ROS levels, and HIF-1 α activity using cardiac myoblast (H9c2 cells) under hypoxic and non-hypoxic conditions.

Methods

Human platelet-rich plasma

Human platelet-rich plasma was purchased from Zenbio, Inc., Durham, North Carolina. An average of 6 10^6 platelets in 40 ml of plasma was supplied.



Langendorff rabbit model of ischemic reperfusion injury

Langendorff heart studies: Twelve male New Zealand White rabbits (3.5 – 4.0 kg, Charles Rivers) were sedated by administering ketamine (25 mg/kg) intramuscularly. A surgical plane of anesthesia was induced by allowing the animal to breathe isoflurane and oxygen. A midline thoracic-abdominal incision was made. The heart was quickly removed and placed into a modified Tyrode solution chilled to 0–4 °C. The heart was mounted as previously described [8]. After mounting, a balloon catheter attached to a pressure transducer was inserted into the left ventricle and inflated.

The occlusion balloon used in this study was custom-made from the fingertips of nitrile gloves and adjusted according to the size of each heart (rabbit weight range: 3.5–4.0 kg). Balloon size was selected empirically based on heart dimensions to achieve effective occlusion.

LVSP and LVDP were recorded continuously through a polyvinyl catheter using a transducer. LVWF was calculated by multiplying (LVSP-LVDP) times heart rate. Balloon inflation pressure was not measured in standardized atmospheric units; instead, it was manually adjusted based on heart size to ensure adequate ventricular loading and occlusion. The preparation was allowed to beat spontaneously and equilibrate for 10 min before initiating the experimental protocol. Closing off the flow through the aortic cannula was used to create global ischemia, which was maintained for 30 minutes with the heart encased in a heated water jacket and maintained at 37°C. Experiments were performed using a NOX-2 or NOX-4 inhibitor. The inhibitor was placed into the Tyrode's media bathing the heart to a final concentration of 10 mM and allowed to perfuse the heart for 10 min before global ischemia was started.

PRP (25 µl) was injected into the left ventricular myocardium 10 minutes after inhibitor administration and 10 minutes before the start of global ischemia. The aortic cannula was reopened at the end of the 30-minute ischemic period, and the heart was reperfused for 60 minutes. Left ventricular pressures were analyzed at 10, 20, and 60-minute intervals during reperfusion. All data are stated as the mean ± SE.

Gap junction formation: Adipose-Derived Stem Cell (ADSC) and H9c2 Co-Culture

Cardiac myoblast cells (H9c2) were purchased from ATCC, and Adipose Derived Stem Cells (ADSC) were purchased from Lonza, Inc. H9c2 monolayers were labeled with 2.5 µM of the cytoplasmic-gap junction permeant calcein orange/red stain (Cell Trace; Molecular Probes/Invitrogen) for 24 hours or 5 µM of the cytoplasmic gap junction impermeant stain chloromethyl fluorescein diacetate (Cell Tracker CMFDA; Molecular Probes/Invitrogen). ADSCs were labeled with a red CD-44 marker for 24 hours. Three separate co-culture experiments were performed. Two sterile 6-well plates were seeded with H9c2 cells (passage 4-10; 1×10^6 cells per well), and two sterile 6-well plates were seeded with ADSCs (passage 5-10; 1×10^6 cells per well). After staining, the cells were co-cultured by trypsinizing the ADSCs, removing them from their wells, and

placing them into a corresponding well with the H9c2 cells. Two milliliters of fresh cell culture media (DMEM) were placed in every well, and the cells were returned to a CO₂ incubator for 24 h. All labeled cells were washed with 1X phosphate-buffered saline (PBS). After staining, the co-cultures were treated with two separate concentrations of PRP (10 µL or 30 µL) for 24 h. Confocal microscopy was performed using a Leica microscope to observe a fluorescent signal in the co-cultured cells.

ROS Assay: A Cellular ROS Fluorometric Assay Kit (red) (Abcam, Waltham, MA, USA) was used to quantify ROS in H9c2 cells. Cells were plated in a 96-well plate (1×10^4 to 4×10^4) on the day before the assay. The cells were exposed to 30 minutes of hypoxia or no hypoxia. Hypoxia was created by placing the cells in an oven heated to 37 °C and flooded with nitrogen gas balanced with 5% CO₂. The ROS Red Working solution was added to each well, and the plate was incubated in a CO₂ incubator for 15 minutes, then immediately analyzed for ROS using a Plate Reader.

HIF-1α Assay: A RayBio® Hydroxylated-HIF-1α (HIF1-α) (Pro402) ELISA Kit was used to measure HIF-1α levels in H9c2 cells in culture. This kit is an *in vitro* enzyme-linked immunosorbent assay used for the measurement of HIF-1α. An anti-pan HIF-1α antibody was coated onto a 96-well plate. Samples were pipetted into the wells, and HIF-1α present in a sample bound to the wells by the immobilized antibody. The wells were washed, and rabbit anti-Hydroxylated-HIF-1α (Pro402) antibody was used to detect Hydroxylated HIF-1α. After washing away the unbound antibody, HRP-conjugated anti-rabbit IgG was pipetted into the wells. The wells were rewashed, and a TMB substrate solution was added to the wells. The color developed was in proportion to the amount of Hydroxylated HIF-1α bound. A Stop Solution was added, and the intensity of the color change was measured at 450 nm using a fluorescent plate reader.

Statistical analysis: The Langendorff Heart data were analyzed using an analysis of variance corrected for repeated measures and presented as a percentage of the baseline value. The Tukey HSD Test was used to determine which, if any, groups were statistically different. The *in vitro* data were analyzed using a student t-test or a one-way analysis of variance. The data are stated as the mean ± SE and considered significant at $p < 0.05$.

Results

LVSP and LVDP in the Langendorff heart model of MIRI

Langendorff Heart Treatment with PRP Alone: Figure 1a illustrates the changes in LVSP and LVDP in hearts treated with PRP and exposed to 30 min of global ischemia and one hour of reperfusion ($n = 4$ hearts). A baseline value was the value established before any treatments were performed and was normalized to 100%. Ten minutes into reperfusion, there was a 27% decrease in LVSP from the baseline value. However, 60 min into reperfusion, LVSP was 25% above the baseline value. LVDP increased significantly above the baseline value at all points during reperfusion, but there was no significant change in LVWF during reperfusion (Figure 1b).



Langendorff heart treatment with a NOX-2 inhibitor and PRP: In a separate group of hearts ($n = 4$), Figure 2a shows the changes in LVSP and LVDP when the NOX-2 inhibitor and PRP were introduced as previously described in the methods section, and the hearts were exposed to 30 min of global ischemia and 1 h of reperfusion. There was a significant increase in both LVSP and LVDP above the baseline values during reperfusion (Figure 2a), but no significant change in LVWF (Figure 2b).

Langendorff heart treatment with a NOX-4 inhibitor and PRP: Figure 3a illustrates the response of LVSP and LVDP to the NOX-4 inhibitor, PRP, 30 min of global ischemia, and one hour of reperfusion. LVSP increased above the baseline value at all time points during reperfusion. Interestingly, LVDP decreased to below the baseline value at the 20- and 60- minute time points during reperfusion. Although the change in LVWF was not quite statistically significant ($p < 0.08$), there was a trend for LVWF to decrease when the NOX-4 enzyme was inhibited (Figure 3b).

Langendorff heart treatment with a NOX PAN inhibitor and PRP: Figure 4a illustrates the response of LVSP and LVDP to PAN NOX inhibition (inhibition of both NOX-2 and NOX-4 simultaneously), PRP, 30 min of global ischemia, and one

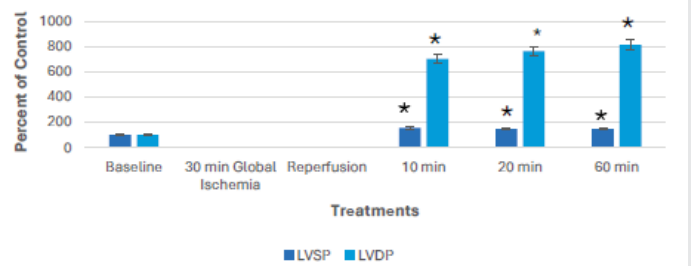


Figure 2a: Left ventricular systolic pressure (LVSP) and left ventricular diastolic pressure (LVDP) in hearts treated with a NOX-2 Inhibitor and platelet-rich plasma (PRP) and exposed to 30 minutes of ischemia and 1 hour of reperfusion. The NOX-2 inhibitor was placed in the Tyrode's media bathing the heart to a final concentration of 10 μ M and allowed to perfuse the heart for 10 minutes before global ischemia was started. PRP was injected into the left ventricular myocardium 10 minutes after the NOX-2 inhibitor was administered and 10 min before the start of global ischemia. LVSP and LVDP increased during reperfusion. Four separate experiments were performed. Data is normalized to the percentage of the baseline. * Represents $p < 0.05$ versus the baseline value.

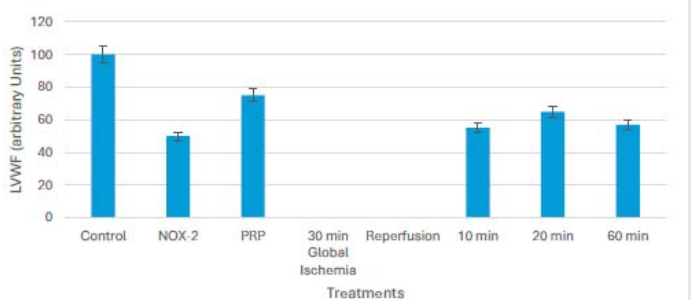


Figure 2b: Left ventricular work function (LVWF) in hearts in Figure 2a treated with a NOX-2 Inhibitor and platelet-rich plasma (PRP), exposed to 30 minutes of ischemia and 1 hour of reperfusion. Work function was calculated by multiplying LVSP times heart rate. Data is normalized to the percentage of the baseline value. There was no significant change in LVWF from the baseline value.

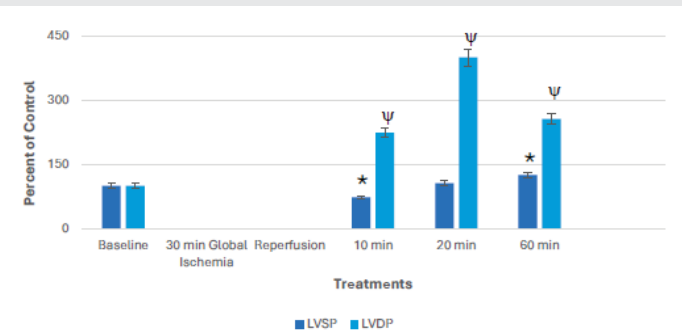


Figure 1a: Left ventricular systolic pressure (LVSP) and left ventricular diastolic pressure (LVDP) in hearts treated with platelet-rich plasma (PRP), exposed to 30 minutes of ischemia and 1 hour of reperfusion. PRP (25 μ l) was injected into the left ventricular myocardium 10 minutes before the start of global ischemia. Left ventricular pressures were analyzed 10,20 and 60-minutes during reperfusion. LVSP was significantly below control 10 minutes into reperfusion but increased to above control at the 60-minute time point. LVDP increased during reperfusion. Four separate experiments were performed. Data is normalized to the percentage of the baseline value. * and Ψ represent $p < 0.05$ versus baseline.

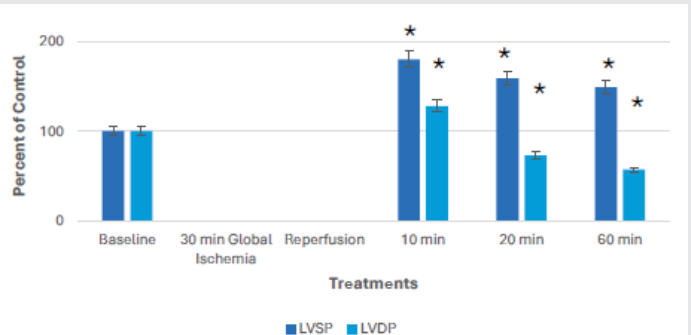


Figure 3a: Left ventricular systolic pressure (LVSP) and left ventricular diastolic pressure (LVDP) in hearts treated with a NOX-4 Inhibitor and platelet-rich plasma (PRP) and exposed to 30 minutes of ischemia and 1 hour of reperfusion. The NOX-4 inhibitor was placed in the Tyrode's media bathing the heart to a final concentration of 10 μ M and allowed to perfuse the heart for 10 minutes before global ischemia was started. PRP was injected into the left ventricular myocardium 10 minutes after the NOX-4 inhibitor was administered and 10 min before the start of global ischemia. LVSP increased significantly above the baseline value at all time points during reperfusion. LVDP was significantly above baseline 10 minutes into reperfusion but decreased significantly to below the baseline value at the 20- and 60-minute time points. Four separate experiments were performed. Data is normalized to the percentage of the baseline value. * Represents $p < 0.05$.

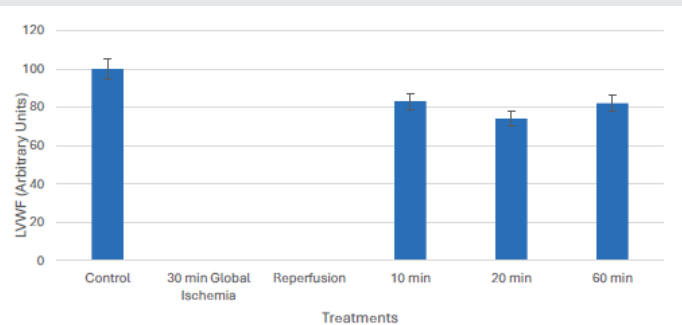


Figure 1b: Left ventricular work function (LVWF) in hearts in Figure 1a treated with platelet-rich plasma (PRP), exposed to 30 minutes of ischemia and 1 hour of reperfusion. Work function was calculated by multiplying (LVSP-LVDP) times heart rate. Data is normalized to the percentage of the baseline value. There was no significant change in LVWF from the baseline value.

hour of reperfusion. Inhibition of both NOX-2 and NOX-4 was associated with a significant decrease in LVSP and an increase in LVDP during reperfusion (Figure 4a). LVWF decreased and

remained below baseline value at the 20- and 60-minute time points during reperfusion (Figure 4b).

In Vitro Studies: All *in vitro* studies were performed using cardiac myoblast (H9c2 cells) and/or adipose-derived stem cells (ADSC) in culture.

Co-culture of H9c2 and ADSCs in the presence of PRP

These studies were performed to investigate the effects of PRP on the formation of channels or pathways between H9c2 and ADSC. Figures 5a through 5d are representative examples of the change in fluorescent color in the co-cultured cells. Calcein is a cell-permanent dye that can move from the H9c2 cell into the ADSC. CMFDA (chloromethyl fluorescein diacetate) is a cytoplasmic gap junction impermeant dye. The yellowish-green fluorescence observed suggests dye movement from the H9c2 cells into the ADSCs. Figure 5a illustrates the yellowish-green change in fluorescence in cells treated with calcein and 10 μ l of PRP. Figure 5b shows no yellowish-green change in fluorescence in cells treated with CMFDA and 10 μ l PRP. Cells treated with 30 μ l of PRP and stained with calcein (Figure 5c) showed a greater degree of yellowish-green fluorescence and

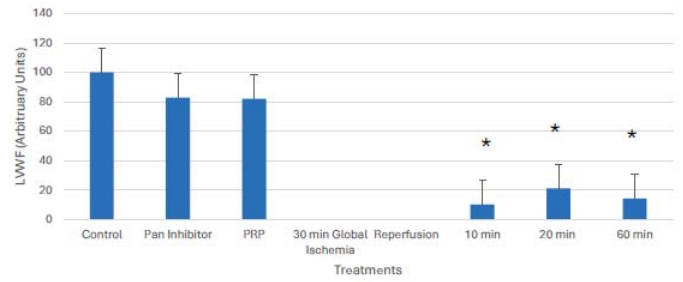


Figure 4b: Left ventricular work function (LVWF) in hearts in Figure 4a treated with the NOX Inhibitors and platelet-rich plasma (PRP), exposed to 30 minutes of ischemia and 1 hour of reperfusion. Work function was calculated by multiplying (LVSP-LVDP) times heart rate. Data is normalized to the percentage of the baseline value. LVWF decreased significantly 20-60 minutes into reperfusion. * Represents $p < 0.05$ versus the baseline value.

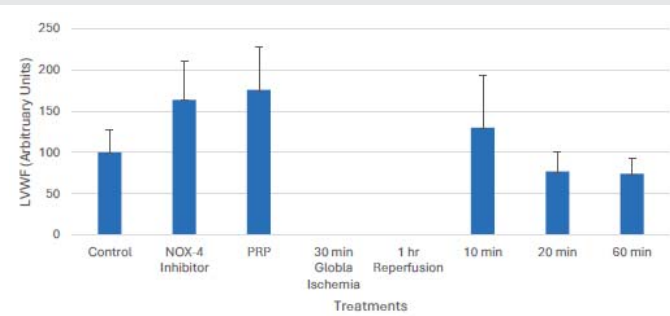


Figure 3b: Left ventricular work function (LVWF) in hearts in Figure 3a treated with a NOX-4 Inhibitor and platelet-rich plasma (PRP), exposed to 30 minutes of ischemia and 1 hour of reperfusion. Work function was calculated by multiplying (LVSP-LVDP) times heart rate. Data is normalized to the percentage of the baseline value. Although there was no statistically significant change in LVWF from the baseline value, LVWF decreased at the 20- and 60-minute time points during reperfusion ($p < 0.08$).

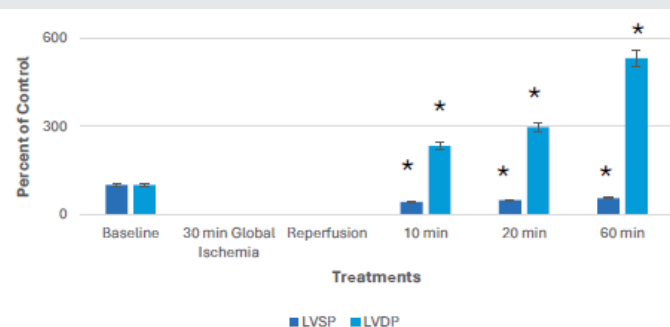


Figure 4a: Left ventricular systolic pressure (LVSP) and left ventricular diastolic pressure (LVDP) in hearts treated with both NOX-2 and NOX-4 Inhibitors, simultaneously, and platelet-rich plasma (PRP) and exposed to 30 minutes of ischemia and 1 hour of reperfusion. The NOX inhibitors were placed in the Tyrode's media bathing the heart to a final concentration of 10 μ M and allowed to perfuse the heart for 10 minutes before global ischemia was started. PRP was injected into the left ventricular myocardium 10 minutes after the NOX inhibitors were administered and 10 min before the start of global ischemia. LVSP and LVDP increased during reperfusion. Four separate experiments were performed. Data is normalized to the percent of control. * Represents $p < 0.05$ versus the baseline value.

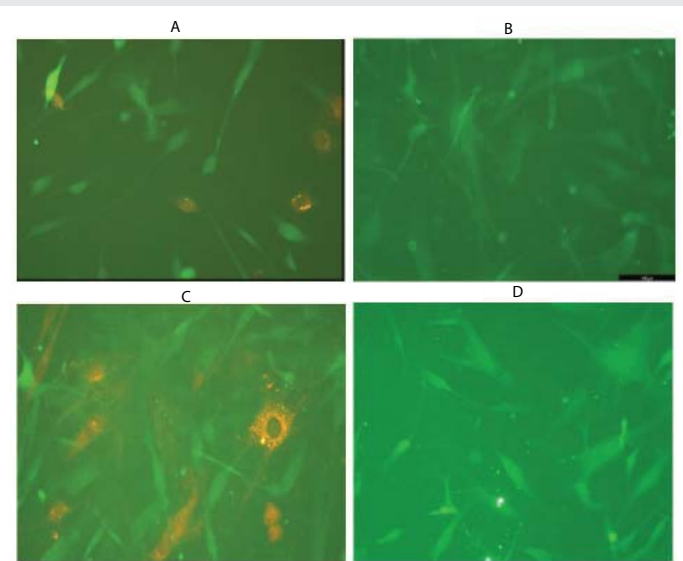


Figure 5a-d: H9c2 cells and ADSCs were co-cultured and stained with calcein or CMFDA and treated with 10 μ l or 30 μ l of PRP. Three separate experiments were conducted. H9c2 cells were labeled with 2.5 μ M of the cytoplasmic-gap junction permeant calcein dye or 5 μ M of the cytoplasmic gap junction impermeant chloromethyl fluorescein diacetate (CMFDA). ADSCs were labeled with the marker CD-44.

no change in fluorescence in the cells stained with CMFDA (Figure 5d). The data suggest the formation of a channel or pathway between the H9c2 and ADSC cells. These channels may serve as a mechanism used by PRP to support left ventricular function during MIRI, which is to enhance the propagation of electrical activity in the damaged heart, and are supported by our previously published data [11].

ROS levels in H9c2 cells in culture exposed to hypoxia or normoxia

Cultured H9c2 cells were exposed to hypoxia or non-hypoxia and treated with PRP or an NOX-2 or NOX-4 Inhibitor or both NOX-2 and NOX-4 Inhibitors: In these experiments, we investigated the effects of PRP on ROS production under hypoxic or non-hypoxic conditions using H9c2 cells in culture treated with PRP (5 μ L, 10 μ L, or 15 μ L) and a NOX-2 (10 μ M) inhibitor or a NOX-4 (10 μ M) inhibitor, or PRP with both the NOX-2 and NOX-4 inhibitors, simultaneously. (In this work,



when both the NOX-2 and NOX-4 inhibitors are administered together, they are referred to as a PAN inhibitor.

Baseline ROS Concentrations in Hypoxic and Non-hypoxic H9c2 Cells: Figure 6 shows the baseline ROS levels in the cells exposed to 30 min of hypoxia or no hypoxia. Under baseline conditions, the ROS levels were 132% higher in hypoxic than in the non-hypoxic cells (Figure 6).

The ROS Response to PRP and the NOX-2 Inhibitor: Figure 7 shows the response of H9c2 cells to PRP under hypoxic or non-hypoxic conditions. PRP significantly reduced ROS levels in the hypoxic but not in the non-hypoxic cells (Figure 7). PRP also decreased ROS levels in the non-hypoxic cells, but the change was not statistically significant.

The ROS Response to PRP and the NOX-2 Inhibitor: Figure 8 shows the ROS response to PRP in the presence of the NOX-2 inhibitor. There was a significant decrease in ROS from the control value with all doses of PRP in the hypoxic cells. There was a tendency for ROS levels to increase from the control value in non-hypoxic cells, but the change was not significant (Figure 8).

The ROS Response to PRP and the NOX-4 Inhibitor: Figure 9 shows the ROS response to PRP when the NOX-4 inhibitor was administered. There was a significant decrease in ROS from the control value with all doses of PRP in the hypoxic cells. There was a tendency for ROS levels to increase from the control value in non-hypoxic cells, but the change was not significant (Figure 9).

The ROS Response to PRP and Inhibition of both NOX-2 and NOX-4 (PAN Inhibitor): Figure 10 shows changes in ROS levels with the inhibition of both NOX-2 and NOX-4 simultaneously. There was a tendency for ROS levels to increase from the control value in non-hypoxic cells, but the change was not significant (Figure 10).

PRP and HIF-1α Activity

In separate experiments, we investigated the effects of PRP on HIF-1α levels in H9c2 cells. In the non-hypoxic cells, there was a 98% decrease in HIF-1α activity from the positive control (Figure 11). However, in the hypoxic cells, there was only a 33, 23, and 22% decrease in HIF-1α levels, respectively, from the positive control in response to 5 ml, 10 ml, or 15 ml of PRP (Figure 11).

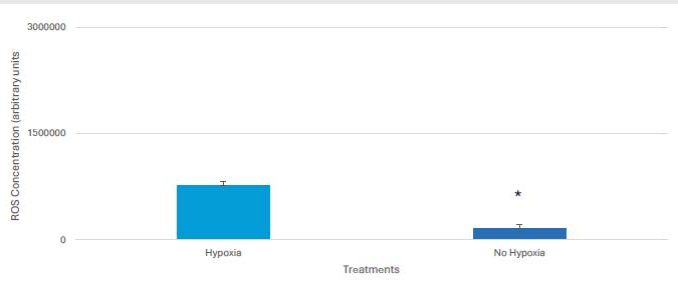


Figure 6: The ROS concentration in H9c2 cells exposed to 30 min of hypoxia or no hypoxia. Eleven separate experiments were conducted. The baseline ROS level was significantly lower in the non-hypoxic cells than in the cells exposed to hypoxia. Data are stated as the mean ± SE. ROS levels were analyzed using a student t-test. * Represents $p < 0.05$ and is considered statistically significant.

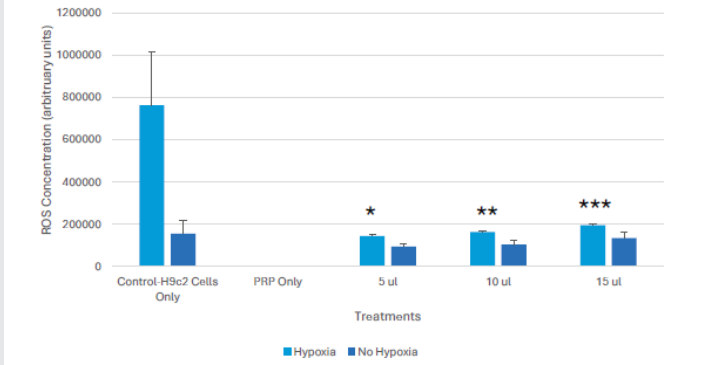


Figure 7: The ROS concentration in H9c2 cells exposed to 30 min of hypoxia or no hypoxia and treated with three different doses of PRP. Eleven separate experiments were performed. Data are stated as the mean ± SE. ROS levels were analyzed using a student t-test. ROS levels decreased significantly ($*p < 2.4e-12$ $**p < 2.8e-12$, $***p < 4.9e-12$) from the baseline value in the cells exposed to hypoxia, but did not decrease significantly from the control value in the non-hypoxic cells.

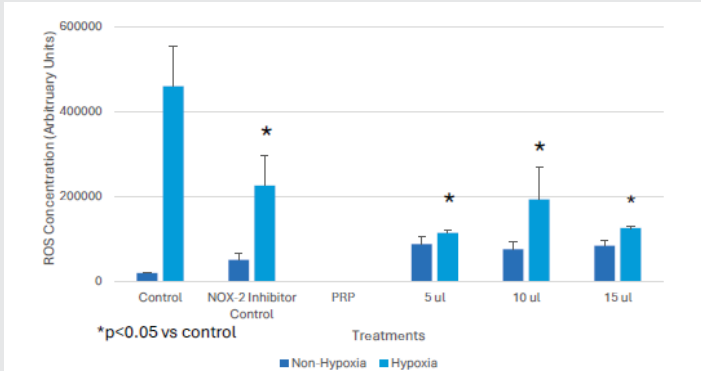


Figure 8: The ROS concentration in H9c2 cells exposed to 30 min of hypoxia (n = 7) or no hypoxia (n = 10) and treated with a NOX-2 inhibitor. The NOX-2 inhibitor alone significantly decreased ROS levels below the control value in the hypoxic cells. There was a further decrease in ROS levels when the cells were treated with three different concentrations of PRP. ROS levels were analyzed using one-way ANOVA with post hoc Tukey tests. Data is stated as the mean ± SE. * represents $p < 0.05$ versus the baseline value. ROS levels in the non-hypoxic cells did not change significantly from the baseline value.

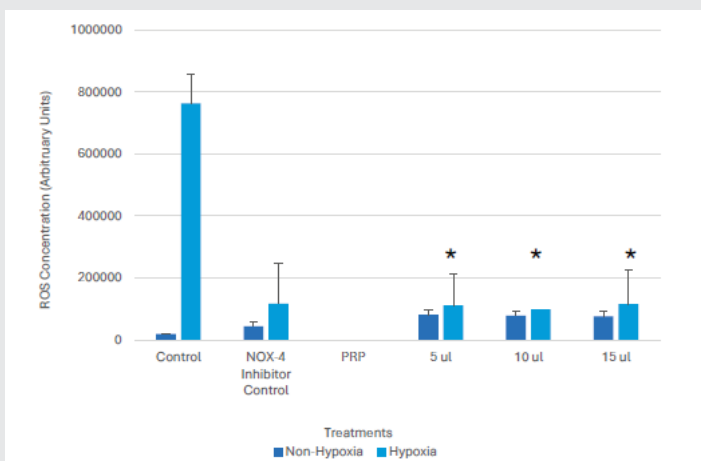


Figure 9: The ROS concentration in H9c2 cells exposed to 30 min of hypoxia (n = 7) or no hypoxia (n = 10) and treated with a NOX-4 inhibitor and PRP. The NOX-4 inhibitor alone significantly decreased ROS levels below the baseline ($p < 7.9e-12$) value in the hypoxic cells. The decrease in ROS was maintained in response to the three different concentrations of PRP administered. There was no significant change in ROS levels in the non-hypoxic cells from the baseline value. ROS levels were analyzed using one-way ANOVA with post hoc Tukey tests. Data is stated as the mean ± SE.

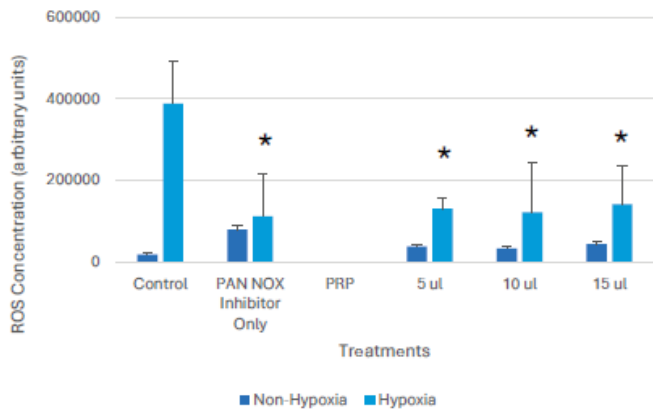


Figure 10: ROS concentration in H9c2 cells exposed to 30 min of hypoxia ($n = 7$) or no hypoxia ($n = 10$) and treated with a NOX-2 and NOX-4 inhibitor (PAN inhibitor) and PRP. The NOX-PAN inhibitor alone decreased ROS levels below the control value in the hypoxic cells. ROS levels remained significantly below the control value with the addition of PRP. ROS levels in the non-hypoxic cells did not change significantly from the control value. ROS levels were analyzed using one-way ANOVA with post hoc Tukey tests. Data is stated as the mean \pm SE. * represents $p < 0.05$ versus the baseline value.

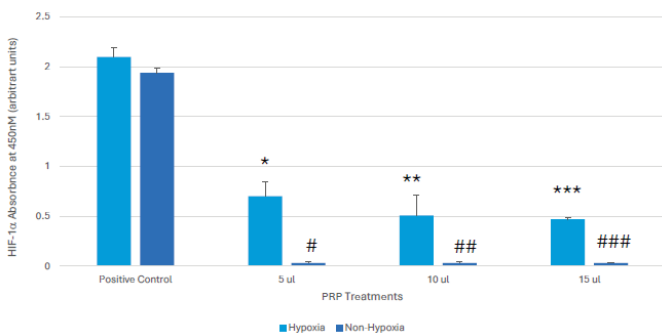


Figure 11: The HIF-1 α activity in H9c2 cells under hypoxic ($n = 3$) or non-hypoxic ($n = 7$) conditions and treated with PRP. There was a dose-dependent decrease in HIF-1 α activity from the positive control baseline values in the hypoxic cells (* $p < 0.03$, ** $p < 0.01$, and *** $p < 0.004$) and in the non-hypoxic cells (# $p < 1.6e-6$, ## $p < 1.9e-6$, and ### $p < 2.4e-7$) in response to the three different concentrations of PRP. Data was analyzed using a student t-test. Data are stated as the mean \pm SE.

Discussion

PRP is an attractive potential therapeutic agent for the treatment of MIRI because of its unique composition and wealth of bioactive molecules that aid in repairing damaged or wounded tissues.

Several investigators have reported on the efficacy of PRP in ischemic heart disease. Gallo et al reported that PRP increased the formation of new vessels [30]. Mishra, et al. showed that PRP was associated with a higher left ventricular ejection fraction [31] while Vu, et al. reported attenuated adverse cardiac remodeling [32]. Yu, et al. reported a decreased infarct size [33], and Sun, et al. described an overall improved LV performance [34]. Our laboratory previously reported that electrical activity returned to the left ventricle faster in the rabbit Langendorff model of MIRI in hearts treated with PRP than in hearts treated with vehicle [11]. The mechanism used by PRP to accomplish many of these changes is still unclear. One aim of the present study was to investigate whether PRP requires the NADPH oxidases

NOX-2 and/or NOX-4 to support left ventricular heart function after ischemia during reperfusion. As reported by Dil, et al. [29], the no-reflow phenomenon is thought to be associated with an increase in LVDP pressure, which causes damage to the coronary microvasculature [29]. The data presented in this study, using the Langendorff model of MIRI, showed an increase in LVDP during reperfusion with PRP treatment alone and with PRP treatment and inhibition of the NOX-2 enzyme.

However, the increase in LVDP was less in the PRP-treated hearts without inhibition of NOX-2 (only a 156% increase) compared to the increase observed in the hearts treated with PRP and inhibition of the NOX-2 enzyme (716% increase). It is worth noting that left ventricular work function did not change significantly during reperfusion with either PRP treatment alone or when PRP was used, and the NOX-2 enzyme was inhibited. Collectively, the Langendorff heart data coupled with the *in vitro* data showing a decrease in ROS levels in response to PRP suggest that PRP may have reduced the level of ROS to an extent that the cardiac myocytes could defend themselves against extensive damage and thereby maintain left ventricular function. Sixty minutes into reperfusion, LVWF was only 18% below the control value in the hearts treated with PRP alone (with the NOX enzymes intact) compared to the 43% drop in LVWF at the same time point with PRP treatment and inhibition of the NOX-2 enzyme. There was only a 25% increase in LVSP in the hearts treated with PRP alone 60 minutes into reperfusion, compared to a 46% increase observed in the hearts with inhibition of the NOX-2 enzyme at the same time point during reperfusion. Without the NOX-2 enzyme, the heart had to generate greater systolic pressure to keep LVWF from falling significantly. While the NOX-2 enzyme appears to be necessary, its interaction with PRP remains unclear.

The administration of PRP and the NOX-4 inhibitor was associated with a decrease in LVDP during reperfusion. Sixty minutes into reperfusion, LVDP was 43% below the baseline value, while LVSP increased 49%. Unlike the NOX-2 enzyme, which is inducible, NOX-4 is constitutively secreted and is regulated by the levels of expression. We theorize that in the absence of the NOX-4 enzyme, PRP can further reduce ROS to levels that allow the antioxidant systems to stabilize LVDP during reperfusion; however, further research is needed. The NOX-4 enzyme may be a therapeutic target for PRP or other agents to reduce LVDP and minimize damage to the coronary microvascular during reperfusion and reduce the occurrence of the no-reflow phenomenon. Although there was no significant change in LVWF, there was a strong tendency for LVWF to decrease at the 20- and 60- minute time points. One possible explanation is that without the ROS contributed by the NOX-4 enzyme and the reduction in ROS associated with PRP, ROS levels fall below that needed for activation of signaling pathways, such as the Nrf2 pathway, which support heart function. Secondly, the increase in LVSP observed with inhibition of the NOX-4 enzyme was not sufficient to maintain LVWF after 60 minutes of reperfusion. LVWF was 74% below the baseline value at the 60-minute time point during reperfusion.

With inhibition of both the NOX-2 and NOX-4 enzymes in the Langendorff hearts, LVDP increased, and LVWF decreased



significantly. Which NADPH oxidase, NOX-2 or NOX-4, is more important to the mechanism of action of PRP remains to be determined.

The *in vitro* data obtained using H9c2 cells in culture show that PRP decreases ROS levels during hypoxia but not in non-hypoxic cells, data that is consistent with previous studies. It is worth noting that there was a tendency for ROS to increase in non-hypoxic cells treated with PRP. It is unclear why PRP was associated with increases in ROS in normoxic but not in hypoxic cells. It is possible that the high.

Concentrations of growth factors contained within PRP can stimulate cellular metabolism and ROS production under non-hypoxic conditions.

In this study, we showed that PRP is associated with the formation of pathways that allow the passage of dye from H9c2 cells in culture into ADSC in a dose-dependent manner, suggesting the presence/formation of channels. The formation of channels between the cells may account for the faster return of electrical activity after ischemia and reperfusion in the PRP-treated hearts we previously reported [11]. Whether PRP drives the development of new channels or activates channels (other than voltage-gated channels) that are already present in cardiomyocytes is unclear. Of particular interest is the presence of Piezo1 channels in the heart. Piezo1 channels are a family of mechanosensitive ion channels that transduce mechanical forces into cellular signals [37]. The discovery of these channels by Coste, Mathur, and Schmidt was recognized in the 2021 Nobel Prize for Physiology or Medicine [38]. The Piezo1 and Piezo 2 membrane proteins form calcium-permeable nonselective cation channels activated by mechanical force sensing in the heart [39]. The activation of Piezo1 is associated with the movement of calcium into the cell. Novosolova et al report that Piezo1 activity is reduced under conditions of oxidative stress [40]. A question for future study is whether the ability of PRP to lower ROS during hypoxia increases the activity of the Piezo1 channel, allowing more calcium to enter the myocyte, thereby improving contractility.

The mechanism by which PRP supports the heart remains open for study. Our *in vitro* data measuring HIF-1 α in H9c2 cells exposed to hypoxia suggest that PRP may help stabilize the upregulated levels of HIF-1 α stimulated by hypoxia so that it is not readily degraded and can maintain cell energy by turning on glycolytic genes and inhibiting apoptotic genes in support of cell survival. We have previously reported that PRP reduced mitochondrial depolarization in H9c2 and HUV-EC (human umbilical cord endothelial cells) in culture stimulated with hydrogen peroxide and analyzed using flow cytometry, suggesting that a decrease in ROS is associated with less damage to the mitochondria [7].

We have also shown that oxygen consumption rates (OCR) measured in real time under basal conditions and in response to indicated mitochondrial inhibitors using the XF^e24 Seahorse Analyzer.

[11] showed that the spare respiratory capacity (a measure of the cell's ability to respond to increased energy demand) and

ATP production were greater in the cells treated with PRP than in the controls [11]. Since PRP has a wealth of growth factors, it is also possible that growth factors, such as PDGF, VEGF, and many others, activate the HIF-1 α pathway to increase HIF-1 α protein levels, which PRP then stabilizes. HIF-1 α levels in the normoxic cells were significantly lower than those observed in the hypoxic cells.

We conclude that in the heart, PRP appears to need NOX-2 and NOX-4 enzymes to maintain a certain level of left ventricular work function during reperfusion, but may be able to modulate their activity via controlling ROS production in myocytes. The control of ROS production may also serve to regulate HIF-1 α activity under hypoxic conditions. In addition, PRP may enhance the formation of gap junctions under hypoxic conditions, thereby supporting electrical activity in the heart.

Ethics approval

The protocol used in all animal studies was approved by the Animal Care and Use Committee at Old Dominion University and per the Guide for the Care and Use of Laboratory Animals, eighth edition, 2011 National Research Council.

Credit authorship contribution statement

Barbara Hargrave, writing, original draft, project administration, methodology, investigation, funding acquisition, conceptualization, surgery and experimentation, software. Frank Lattanzio, resource acquisition, experimentation, methodology, investigation, editing of Langendorff heart data, and software.

References

1. Eltzschig HK, Eckle T. Ischemia and reperfusion—from mechanism to translation. *Nat Med.* 2011;17:1391-1401. Available from: <https://doi.org/10.1038/nm.2507>
2. Ebrahimi S, Esfahani SA, Kohkiloeezadeh M, Moghaddam BH, Askarian S, Tanideh N, Tamadon A. A model of cerebral ischemia induction in neonatal rabbits. *JAAR.* 2021;40:37-42.
3. Piper HM, Meuter K, Schafer C. Cellular mechanisms of ischemia-reperfusion injury. *Ann Thorac Surg.* 2003;75:S644-S648. Available from: [https://doi.org/10.1016/s0003-4975\(02\)04686-6](https://doi.org/10.1016/s0003-4975(02)04686-6)
4. Tavakoli F, Ostad SN, Khori V, Alizadeh AM, Sadeghpour A, Azar AD, et al. Outcome improvement of cellular cardiomyoplasty using triple therapy: mesenchymal stem cell, erythropoietin, and vascular endothelial growth factor. *Eur J Pharmacol.* 2013;714:456-463. Available from: <https://doi.org/10.1016/j.ejphar.2013.07.001>
5. Pagliaro BR, Cannata F, Stefanini GG. Myocardial ischemia and coronary disease in heart failure. *Heart Fail Rev.* 2020;25:53-65. Available from: <https://doi.org/10.1007/s10741-019-09831-z>
6. Tognoloni A, Bartolini D, Pepe M, Meo A, Parcellato I, Guidoni K, et al. Platelet-rich plasma increases antioxidant defenses of tenocytes via the Nrf2 signalling pathway. *Int J Mol Sci.* 2023;24(17):13299. Available from: <https://doi.org/10.3390/ijms241713299>
7. Hargrave BY. Autologous platelet-rich plasma (platelet gel): an appropriate intervention for salvaging cardiac myocytes under oxidative stress after myocardial infarction. *Anat Physiol.* 2014;4(1):1-8. Available from: https://digitalcommons.odu.edu/cgi/viewcontent.cgi?article=1129&context=bioelec_trics_pubs



8. Hargrave B, Li F. Nanosecond pulse electric field activation of platelet-rich plasma reduces myocardial infarct size and improves left ventricular mechanical function in the rabbit heart. *J Extra Corpor Technol.* 2012;44(4):198-204. Available from: <https://pmc.ncbi.nlm.nih.gov/articles/PMC4557561/>
9. Matsushima S, Tsutsui H, Sadoshima J. Physiological and pathological functions of NADPH oxidases during myocardial ischemia-reperfusion. *Trends Cardiovasc Med.* 2014;24(5):202-205. Available from: <https://doi.org/10.1016/j.tcm.2014.03.003>
10. Tang XL, Takano H, Rizvi A, Turrens JF, Qiu Y, Wu WJ, et al. Oxidant species trigger late preconditioning against myocardial stunning in conscious rabbits. *Am J Physiol Heart Circ Physiol.* 2002;282(1):H281-H291. Available from: <https://doi.org/10.1152/ajpheart.2002.282.1.h281>
11. Hargrave B, Varghese F, Barabutis N, Catravas J, Zemlin C. Nanosecond pulsed platelet-rich plasma (nsPRP) improves mechanical and electrical cardiac function following myocardial reperfusion injury. *Physiol Rep.* 2016;4(4):e12710. Available from: <https://doi.org/10.14814/phy2.12710>
12. Mosser DD, Caron AW, Bourget L, Meriin AB, Sherman MY, Morimoto RI, et al. The chaperone function of Hsp70 is required for protection against stress-induced apoptosis. *Mol Cell Biol.* 2000;20(19):7146-7159. Available from: <https://doi.org/10.1128/mcb.20.19.7146-7159.2000>
13. Kayama T, Nakazawa T, Thanos A, Morizane Y, Murakami Y, Theodoropoulou S, et al. Heat shock protein 70 (HSP70) is critical for the photoreceptor stress response after retinal detachment via modulating anti-apoptotic Akt kinase. *Am J Pathol.* 2011;178(3):1080-1091. Available from: <https://doi.org/10.1016/j.ajpath.2010.11.072>
14. Ziello JE, Jovin IS, Huang Y. Hypoxia-inducible factor (HIF)-1 regulatory pathway and its potential for therapeutic intervention in malignancy and ischemia. *Yale J Biol Med.* 2007;80(2):51-60. Available from: <https://pubmed.ncbi.nlm.nih.gov/18160990/>
15. Genbacev O, Zhou Y, Ludlow JW, Fisher SJ. Regulation of human placental development by oxygen tension. *Science.* 1997;277(5332):1669-1672. Available from: <https://doi.org/10.1126/science.277.5332.1669>
16. Matsushima S, Sadoshima J. Yin and yang of NADPH oxidases in myocardial ischemia-reperfusion. *Antioxidants (Basel).* 2022;11(6):1069. Available from: <https://doi.org/10.3390/antiox11061069>
17. Endemann DH, Schiffrin EL. Endothelial dysfunction. *J Am Soc Nephrol.* 2004;15(8):1983-1992. Available from: <https://doi.org/10.1097/01.asn.0000132474.50966.da>
18. Burgoyne JR, Madhani M, Cuello F, Charles RL, Brennan JP, Schröder E, et al. Cysteine redox sensor in PKG1alpha enables oxidant-induced activation. *Science.* 2007;317(5843):1393-1397. Available from: <https://doi.org/10.1126/science.1144318>
19. Kleinschnitz C, Grund H, Wingle K, Armitage ME, Jones E, Mittal M, et al. Post-stroke inhibition of induced NADPH oxidase type 4 prevents oxidative stress and neurodegeneration. *PLoS Biol.* 2010;8(9):e1000479. Available from: <https://doi.org/10.1371/journal.pbio.1000479>
20. Braunersreuther V, Montecucco F, Asrih M, Pelli G, Galan K, Frias M, et al. Role of NADPH oxidase isoforms NOX1, NOX2, and NOX4 in myocardial ischemia/reperfusion injury. *J Mol Cell Cardiol.* 2013;64:99-107. Available from: <https://doi.org/10.1016/j.yjmcc.2013.09.007>
21. Matsushima S, Kuroda J, Ago T, Zhai P, Ikeda Y, Oka S, et al. Broad suppression of NADPH oxidase activity exacerbates ischemia/reperfusion injury through inadvertent downregulation of hypoxia-inducible factor-1alpha and upregulation of peroxisome proliferator-activated receptor-alpha. *Circ Res.* 2013;112(8):1135-1149. Available from: <https://doi.org/10.1161/circresaha.111.300171>
22. Siu KL, Lotz C, Ping P, Cai H. Netrin-1 abrogates ischemia/reperfusion-induced cardiac mitochondrial dysfunction via nitric oxide-dependent attenuation of NOX4 activation and recoupling of NOS. *J Mol Cell Cardiol.* 2015;78:174-185. Available from: <https://doi.org/10.1016/j.yjmcc.2014.07.005>
23. Schröder K, Zhang M, Benkhoff S, Mieth A, Pliquett R, Kosowski J, et al. Nox4 is a protective reactive oxygen species-generating vascular NADPH oxidase. *Circ Res.* 2012;110(9):1217-1225. Available from: <https://doi.org/10.1161/circresaha.112.267054>
24. Ago T, Kuroda J, Pain J, Fu C, Li H, Sadoshima J. Upregulation of Nox4 by hypertrophic stimuli promotes apoptosis and mitochondrial dysfunction in cardiac myocytes. *Circ Res.* 2010;106(7):1253-1264. Available from: <https://doi.org/10.1161/circresaha.109.213116>
25. Kloner RA, King KS, Harrington MG. No-reflow phenomenon in the heart and brain. *Am J Physiol Heart Circ Physiol.* 2018;315(3):H550-H562. Available from: <https://doi.org/10.1152/ajpheart.00183.2018>
26. Smyth JW, Hong TT, Gao D, Vogan JM, Jensen BC, Fong TS, et al. Limited forward trafficking of connexin 43 reduces cell-cell coupling in stressed human and mouse myocardium. *J Clin Invest.* 2010;120(1):266-279. Available from: <https://doi.org/10.1172/jci39740>
27. Smyth JW, Shaw RM. The gap junction life cycle. *Heart Rhythm.* 2012;9(1):151-153. Available from: <https://doi.org/10.1016/j.hrthm.2011.07.028>
28. Kaur G, Baghdasaryan P, Natarajan B, Sethi P, Mukherjee A, Varadarajan P, et al. Pathophysiology, diagnosis, and management of coronary no-reflow phenomenon. *Int J Angiol.* 2022;31:107-112. Available from: <https://doi.org/10.1055/s-0041-1725979>
29. Dil S, Ryabov V, Maslov L, Mochula O, Mochula A, Kercheva M, et al. Assessing coronary microvascular dysfunction in refractory no-reflow: insights from dynamic myocardial perfusion scintigraphy and cardiac MRI. *Microvasc Res.* 2025;162:104862. Available from: <https://doi.org/10.1016/j.mvr.2025.104862>
30. Gallo I, Sáenz A, Arévalo A, Roussel S, Pérez-Moreiras I, Artiñano E, et al. Effect of autologous platelet-rich plasma on heart infarction in sheep. *Arch Cardiol Mex.* 2013;83:154-158. Available from: <https://doi.org/10.1016/j.acmx.2013.04.011>
31. Mishra A, Velotta J, Brinton TJ, Wang X, Chang S, Palmer O, et al. RevaTen platelet-rich plasma improves cardiac function after myocardial injury. *Cardiovasc Revasc Med.* 2011;12:158-163. Available from: <https://doi.org/10.1016/j.carrev.2010.08.005>
32. Vu TD, Pal SN, Ti LK, Martinez EC, Rufaihah AJ, Ling LH, et al. An autologous platelet-rich plasma hydrogel compound restores left ventricular structure, function and ameliorates adverse remodeling in a minimally invasive large animal myocardial restoration model: a translational approach. *Biomaterials.* 2015;45:27-35. Available from: <https://doi.org/10.1016/j.biomaterials.2014.12.013>
33. Yu FX, Zhang Y, Tran N, Fu Y, Liao B, Shi YK. Effects of myocardial platelet-rich plasma injection on rats with acute myocardial infarction: 99Tc(m)-MIBI gated SPECT imaging evaluation results. *Zhonghua Xinxue Guanbing Zazhi.* 2012;40:392-396. Available from: <https://scispace.com/papers/effects-of-myocardial-platelet-rich-plasma-injection-on-rats-2qcyk1opjx>
34. Sun CK, Zhen YY, Leu S, Tsai TH, Chang LT, Sheu JJ, et al. Direct implantation versus platelet-rich fibrin-embedded adipose-derived mesenchymal stem cells in treating rat acute myocardial infarction. *Int J Cardiol.* 2014;173:410-423. Available from: <https://doi.org/10.1016/j.ijcard.2014.03.015>
35. Sirker A, Zhang M, Murdoch C, Shah AM. Involvement of NADPH oxidases in cardiac remodeling and heart failure. *Am J Nephrol.* 2007;27(6):649-660. Available from: <https://doi.org/10.1159/000109148>



36. Ago T, Matsushima S, Kuroda J, Zablocki D, Kitazono T, Sadoshima J. The NADPH oxidase Nox4 and aging in the heart. *Aging (Albany NY)*. 2010;2(12):1012-1016. Available from: <https://doi.org/10.18632/aging.100261>
37. Chi S. The role of Piezo1 channels in cardiovascular function: mechanotransduction in the heart and blood vessels. *Series Cardiol Res*. 2025;7(1):1-4. Available from: <https://seriescience.com/wp-content/uploads/2025/03/Piezo1-Channels-in-CV-Function.pdf>
38. Coste B, Mathur J, Schmidt M, Earley TJ, Ranade S, Petrus MJ, et al. Piezo1 and Piezo2 are essential components of distinct mechanically activated cation channels. *Science*. 2010;330(6000):55-60. Available from: <https://doi.org/10.1126/science.1193270>
39. McGrane A, Murray M, Bartoli F, Giannoudi M, Conning-Rowland M, Stewart L, et al. PIEZO force sensors and the heart. *Cold Spring Harb Perspect Biol*. 2026;18(2):a041806. Available from: <https://doi.org/10.1101/cshperspect.a041806>
40. Novosolova N, Braidotti N, Patinen T, Laitinen T, Ciubotaru C, Huttunen KM, et al. Oxidative modulation of Piezo1 channels. *Redox Biol*. 2025;86:103797. Available from: <https://doi.org/10.1016/j.redox.2025.103797>

Discover a bigger Impact and Visibility of your article publication with Peertechz Publications

Highlights

- ❖ Signatory publisher of ORCID
- ❖ Signatory Publisher of DORA (San Francisco Declaration on Research Assessment)
- ❖ Articles archived in worlds' renowned service providers such as Portico, CNKI, AGRIS, TDNet, Base (Bielefeld University Library), CrossRef, Scilit, J-Gate etc.
- ❖ Journals indexed in ICMJE, SHERPA/ROMEO, Google Scholar etc.
- ❖ OAI-PMH (Open Archives Initiative Protocol for Metadata Harvesting)
- ❖ Dedicated Editorial Board for every journal
- ❖ Accurate and rapid peer-review process
- ❖ Increased citations of published articles through promotions
- ❖ Reduced timeline for article publication

Submit your articles and experience a new surge in publication services

<https://www.peertechzpublications.org/submission>

Peertechz journals wishes everlasting success in your every endeavours.